Chapter 5

High pressure studies on some different types of liquid crystalline phase transitions

5.1   Introduction

In chapter 2 we described a technique of measuring the optical path difference of aligned liquid crystal samples as functions of both pressure and temperature. We also reported the temperature variations of order parameter S of systems exhibiting N and SmA phases at various pressures. The optical path difference data is also used for the identification of transition temperatures. Using this technique we have detected the N_1N_d transition in a pure nematogen CP7B at elevated pressures. The pressure-temperature (P-T) phase diagram as well as the temperature variations of order parameter of CP7B at various pressures have been presented in chapter 3. In chapter 4 we have reported a new type of NN transition exhibited by a binary mixture of polar compounds. In this chapter we present the P-T phase diagrams of liquid crystalline systems exhibiting various types of phase transitions.

In chapter 6 we will report a new technique of subjecting liquid crystals to negative pressures. As we will describe in the next section, we have chosen two liquid crystalline materials, viz., CBCC and MCB for *negative* pressure experiments, because of their convenient transition temperatures. The method of generating negative pressures does not allow for the direct measurement of the pressure. We can however estimate the negative pressures by the measured transition temperatures if the dP/dT values are known. With this in mind, we have constructed the P-T phase diagrams of both CBCC and MCB. We also report the P-T phase diagram of a binary mixture exhibiting the reentrant nematic phase.

In our laboratory in the past few years some new types of liquid crystals have been discovered [1,3]. The liquid crystal compounds made up of molecules with a large bent-core (with a bend angle of ~120^0) are known as banana or bow shaped liquid crystal compounds (see section 1.4). Pratibha et al [1] have

reported the phase diagram of binary mixtures of a compound made of banana shaped molecules viz., 1,3-phenylene bis[4-(3-methylbenzoyloxy)] 4′-n-dodecylbiphenyl 4′-carboxylate (BC12) and a compound made of rod shaped molecules viz. 4-biphenylyl 4″-n-undecyloxybenzoate (BO11) exhibiting interesting phase transitions. In a composition range of 4 to 13mol% of the banana compound the binary mixtures exhibit the phase sequence: I - N - SmA_2 - SmA_{2b} [1], where SmA_2 and SmA_{2b} correspond to uniaxial smectic and biaxial smectic respectively (with layer spacing d being twice the molecular length of the rod-like molecule in both the cases). They have identified the low temperature phase as SmA_{2b} through textural observations. They have prepared another system of binary mixtures of banana compound BC12 with a compound having different rod shaped molecules viz., 8OCB. This system of binary mixtures in a certain concentration range exhibits the following phase sequence: I - N- SmA_d - SmA_{db} [2]. We have studied the effect of pressure on this phase sequence in a binary mixture with 14 mol% of BC12.

A pure nematogen, 7(CN)5 (see section 5.34) is known to exhibit a skewed cybotactic type of short-range order, the tilt angle increasing considerably as the temperature is lowered from the NI transition point [4]. We have conducted optical path difference measurements on this compound as a function of temperature at elevated pressures and detected a liquid crystal-liquid crystal phase transition at high pressures. A binary mixture of this compound with a chiral compound exhibits twist grain boundary (TGB) phases viz. TGB_A, $UTGB_c^*$ (see section 1.6) in a certain concentration range [3]. As mentioned in chapter 1, $UTGB_c^*$ phase was reported for the first time by Pramod et al [3] from our laboratory. We present the P-T phase diagram of a binary mixture with 36 wt% of 7(CN)5 exhibiting this phase.

5.2 Experimental

The systems used in the study are: (i) p-cyanophenyl carboxylate (CBCC), (ii) a mixture (MCB) with 30 wt% of 4- octyl-4′-cyanobiphenyl (8CB) and 8OCB (iii) Binary mixture of 27.5 mol% 6OCB with 8OCB which exhibit the re-entrant nematic (N_r) phase. (iv) 4'-butyl-4-heptyl-bicyclohexyl-4-carbonitrile (CCN47), (v) binary mixture of 14 mol% of 1,3-phenylene-bis[4-(3-methylbenzoyloxy)]-4'-n-dodecylbiphenyl-4'-carboxylate (BC12) and 8OCB, (vi) 4'-pentyl-biphenyl-4-

carboxylic acid 2-cyano-4-heptyl-phenyl ester (7(CN)5), (vii) A binary mixture of 4-(2- methyl butyl) phenyl 4' -n –octylbiphenyl-4-carboxylate (CE8) and 7(CN)5. The banana compound BC12 was obtained from Prof. B.K. Sadashiva. CE8 was obtained from BDH limited, 7(CN)5 and CCN47 from Merck. All other compounds were obtained from Messrs. Roche.

We have used the technique of optical path difference measurements (see section 2.2) for the identification of the phase transition temperatures at various pressures of the liquid crystals mentioned above.

5.3   Results and Discussion

5.31 P-T phase diagram of a pure nematogen

The compound CBCC is a pure nematogen with one cyclohexane ring in the core of the molecule (Figure 5.1). The birefringence of CBCC is lower compared to a nematogen with 2 phenyl rings.

CBCC
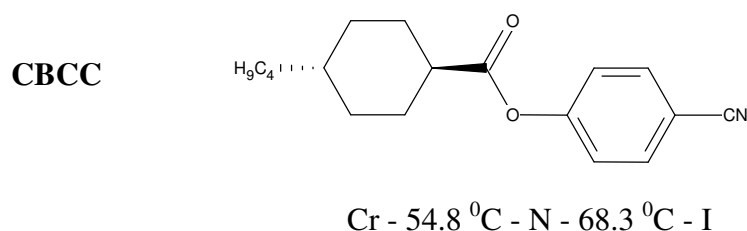
$$Cr - 54.8 \,^0C - N - 68.3 \,^0C - I$$

Figure 5.1: Chemical structure and the transition temperatures of the compound CBCC.

The P-T phase diagram of CBCC pertaining to NI transition is shown in Figure 5.2. The value of dP/dT_{NI} = 24 bar/^{0}C. The values of the heat of transition ΔH (= 0.57 KJ/mole) [5] and the jump in the density $(\Delta\rho_{NI} = 3.06 \times 10^{-3}$ g/cc) [6] at the NI transition for CBCC are available in the literature. Using the Claussius-Clapeyron equation viz., $(dP/dT) = \Delta H/(\Delta V.T_{NI})$, we obtain dP/dT_{NI} = 19 bar/^{0}C which is somewhat lower than the experimental value.
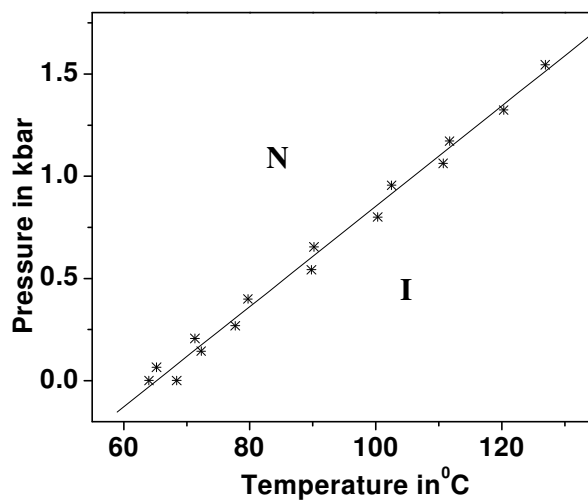
Figure 5.2: The pressure-temperature phase diagram corresponding to the NI transition of CBCC.

5.32 P-T phase diagram of a binary mixture exhibiting smectic A and nematic phases

Many compounds exhibit the phase sequence: I - N - SmA. To conduct negative pressure experiments (to be explained in next chapter) systems exhibiting the N-SmA transition in a convenient temperature range was required. Though 8CB shows the phase sequence, the SmA_d-N transition temperature is 32 ^{0}C, which is very low, and for 8OCB the NI transition temperature is ~80 ^{0}C which is too high for the technique to be adopted for generating negative pressures.

8CB

Cr - 21 ^{0}C - SmA_d - 32.5 ^{0}C - N - 40 ^{0}C - I

8OCB

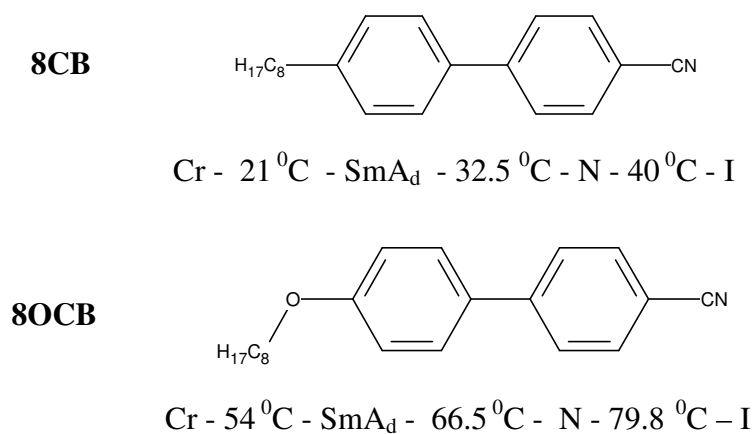Cr - 54 ^{0}C - SmA_d - 66.5 ^{0}C - N - 79.8 ^{0}C – I

Figure 5.3: Chemical structures and the transition temperatures of 6OCB and 8OCB.

We have prepared the binary mixture (MCB) of 8OCB with 30 wt% of 8CB which has a phase transition sequence: SmA_d - 57.8 ^{0}C - N- 70 ^{0}C - I. The SmA_d-N transition occurs at a convenient temperature for negative pressure experiments (see chapter 6). The P-T phase diagram of MCB is shown in Figure 5.4, in which the SmA_d to N and NI phase transition temperatures are plotted as functions of pressure. The slopes dP/dT at the NI and SmA_d-N transitions are 36.8 bar/^{0}C and 71.5 bar/^{0}C respectively. The differential scanning calorimeter peak at the NI transition yields ΔH_{NI} = 2.4J/g. The estimated value of the jump in the density $\Delta\rho_{NI}$=1.8 ×10^{-3} g/cc [7]. The value of dP/dT$_{NI}$ calculated using the Clausius-Clapeyron equation is 39.9 bar/^{0}C, in reasonable agreement with the experimental value.
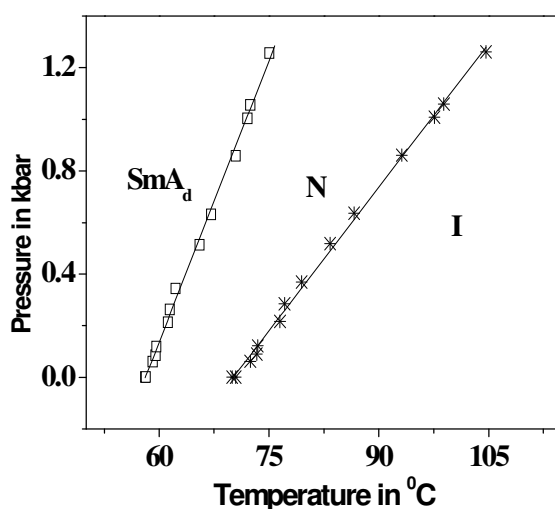

Figure 5.4: The pressure-temperature phase diagram of MCB.

5.33 P-T phase diagram of a binary mixture exhibiting reentrant nematic phase

The binary mixtures of 6OCB and 8OCB exhibit N-SmA_d-N_r phase sequence in a narrow range of concentrations of 6OCB. Guillon et al [8] were the first to construct the phase diagram of the 8OCB-6OCB mixtures as a function of concentration. The concentration-temperature phase diagram is shown in Figure 5.6 (adapted from reference [9]). As the N-SmA_d and SmA_d-N_r transitions occur at relatively low temperatures, mixtures of these compounds have been studied extensively.

6OCB
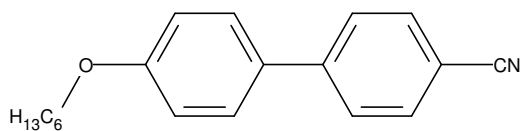
$$Cr - 58\,^0C - N - 76.5\,^0C - I$$

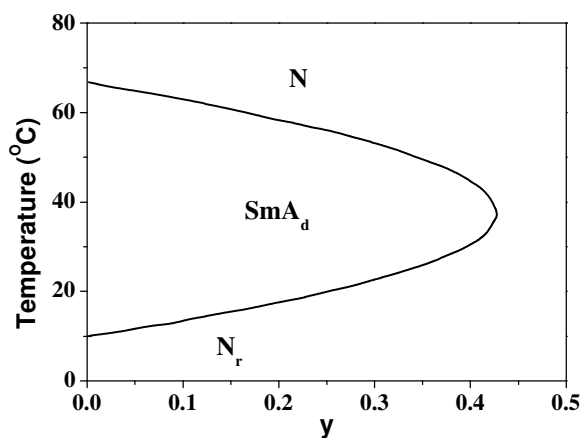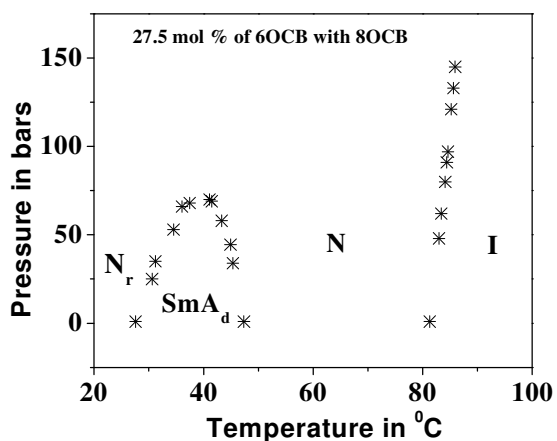Figure 5.5: Chemical structure and transition temperatures of 6OCB.

Figure 5.6: The phase diagram for 6OCB-8OCB mixture as a function of concentration. The concentration **y** is the molecular ratio 6OCB:8OCB (taken from reference [9]).

Figure 5.7: The pressure –temperature phase diagram of 27.5 mol% of 6OCB with 8OCB.

The P-T phase diagram of the binary mixtures has been reported by Cladis et al [10]. The value of P_m, the maximum pressure up to which the SmA_d phase is stable decreases with increasing concentration of 6OCB [10]. The value of P_m is ~ 2.3 kbars for pure 8OCB (see section 2.3). We have constructed the P-T phase diagram for a mixture with 27.5 mol% of 6OCB, and as expected, the SmA_d phase gets suppressed beyond ~75 bars as shown in Figure 5.7. The value of $dP/dT_{NI} = 31$ bar/ ^{0}C.

5.34 Pressure generation in HP cell when a sample is mounted in a fluid state

The liquid crystal compound, CCN47 with a large negative dielectric anisotropy has the following phase transition sequence: Cr - 28 ^{0}C - SmA - 30.6 ^{0}C - N - 59.7 ^{0}C - I (see Figure 5.8). This compound has a very low birefringence value viz. $\Delta\mu$ ~ 0.035 at 30 ^{0}C [11]. This compound as well as the previous sample (see section 5.33) are in a mesophase which is fluid, at room temperature.

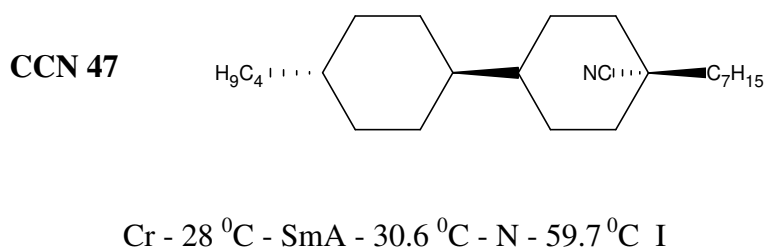Cr - 28 ^{0}C - SmA - 30.6 ^{0}C - N - 59.7 ^{0}C I

Figure 5.8: Chemical structure and transition temperatures of CCN47.

The method of mounting the sample in the HP cell is as follows. One of the pretreated fused quartz cylinders is snugly fit in the fluran tube and a mylar spacer cut in circular shape is placed on top of the fused quartz cylinder. The sample in the fluid form is filled in the circular gap of the mylar spacer. The other pretreated fused quartz is pressed from the top such that the sandwich of the two fused quartz cylinders is snugly fit into the fluran tube. Then as described in chapter 2 (section 2.25) steel wires are wrapped on the fluran tube around both the fused quartz windows to isolate the sample from the pressure transmitting fluid. The sample is mounted in the HP setup along with the other accessories as described in section 2.2 (see Figure 2.2).
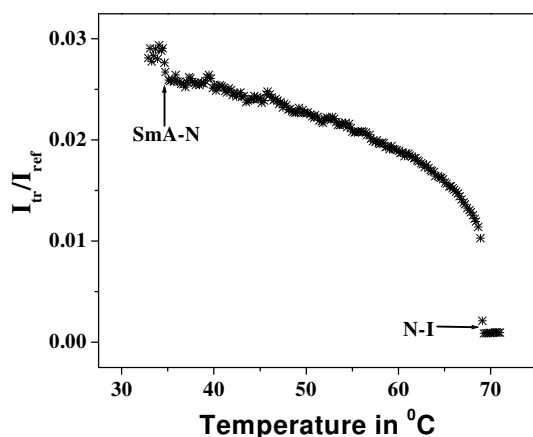
Figure 5.9: Temperature variation of the ratio of transmitted intensity to reference intensity for a sample of CCN47 mounted in HP cell without the application of an external pressure.

The temperature variation of the ratio of transmitted intensity to reference intensity of a planar aligned sample of CCN47 mounted in the HP cell without the application of an external pressure is shown in Figure 5.9. It can be noted that the NI transition occurs at a temperature $\sim$ 69.3 ^{0}C which is about 10 ^{0}C higher than that measured at atmospheric pressure. The SmA-N transition temperature has also increased to $\sim$35.2 ^{0}C. On application of external pressure of $\sim$1 kbar, the T_{NI} and T_{SmAN} further increase to $\sim$ 96.5 ^{0}C and 45 ^{0}C respectively.
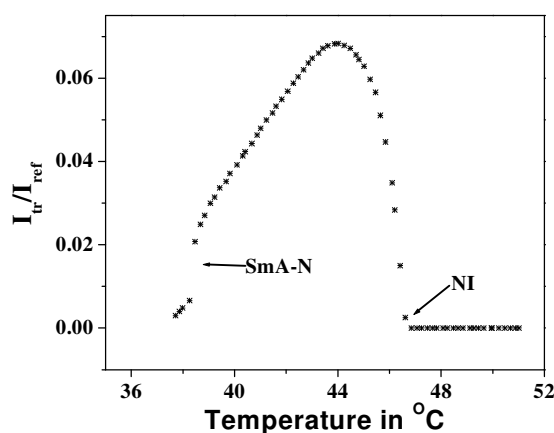

Figure 5.10: Temperature variation of the ratio of transmitted intensity to reference intensity for 8CB.

Thus even in the absence of an external pressure, the liquid crystal medium in the HP cell has developed a high pressure, whose value depends on temperature. This is related with the fluid nature of the material when it is mounted in the HP cell. We also carried out measurements on 8CB with the phase transition sequence: SmA_d - 32.5 ^{0}C - N - 40 ^{0}C - I. We observed that for a planar aligned sample mounted in the HP cell in the absence of any external pressure the transitions again occurred at higher temperatures: T_{SmAN} and T_{NI} were 38.2 ^{0}C and 46.5 ^{0}C respectively (Figure 5.10).

In the case of samples which are mounted in the HP cell by packing powdered crystals at room temperature, enough space is available for the volume to increase at the melting point. But in case of samples which are room temperature mesogens (fluids) the sample occupies the whole space including the gap between the fluran tube and the fused quartz cylinders. As the volume is fixed due to the constraining walls of the high pressure chamber (see Figure 2.2), on heating the sample the *pressure* in the medium raises. Hence the transition temperatures also increase because of the excess pressure even though externally no pressure has been applied to the sample. The effect obviously increases at high temperatures. We also prepared samples with a very small amount of the room temperature liquid crystal 8CB allowing enough space for the volume change to occur at the NI transition. Indeed, we observed that both NI and SmA-N phase transitions occurred at the expected temperatures. But if we adopt this procedure, on application of high pressures the sample sandwiched between fused quartz cylinders leaks out at high temperatures into the crevices between the sandwich and the fluran tube due to capillary forces. There will be no sample between the fused quartz cylinders in the optical path of the laser beam to carry out any optical path difference measurements on the sample.

The compressibility of the medium is $\beta = -(1/V)(dV/dP)$ and the thermal expansion coefficient is $\alpha = (1/V)(dV/dT)$. For compensation of $|\Delta V/V|$, $\beta\Delta P = \alpha\Delta T$. For a typical mesogen the values of α and β are 10×10^{-4} /^{0}C and 10×10^{-12} cm^2 dyne^{-1} respectively [12]. Assuming ΔT to be the temperature difference between the transition temperature and the room temperature (temperature at which

the sample is mounted in the HP cell), the excess pressure ΔP can be estimated. At the NI transition point of 8CB the estimated pressure ΔP ~150 bars. The value of dP/dT_{NI} is typically ~30 bar $/^0C$, hence an increase in T_{NI} ~ 5 ^0C can take place. In case of CCN47 as the value of ΔT is ~ 35 ^0C, the value of ΔP is ~300 bars which can lead to an increase in T_{NI} ~10 ^0C. As mentioned in section 2.2 the line pressure is measured by a Bourdan type (HEISE) gauge (Figure 2.4). Therefore the *actual* pressure experienced by the room temperature liquid crystals mounted in the HP cell will be the *sum* of the pressure generated by the procedure mentioned above and the line pressure measured by the Bourdan gauge. After releasing the external pressure i.e. when the line pressure measured by Bourdan gauge is 1bar, the transition temperatures remain at the same high values as measured before application of external pressure indicating that the pressure generated in the medium will be present throughout.

5.35 P-T phase diagram of a binary mixture of a rod-like mesogen and a banana-shaped mesogen exhibiting biaxial SmA phase

As mentioned in section 5.1 Pratibha et al [2] have reported that a binary mixture of BC12, a banana shaped compound (see Figure 5.11) and a compound with rod-like molecules 8OCB (see Figure 5.3) exhibits a variety of interesting phase transitions (see Figure 5.12). In a narrow range of concentrations of 10 to 24 mol% of BC12 the binary mixtures exhibit the biaxial Smectic A phase (Figure 5.12). Through X-ray studies the authors have confirmed that the rods form a partial bilayer structure of 8OCB molecules in the SmA_{db} phase in this binary mixture.

BC12
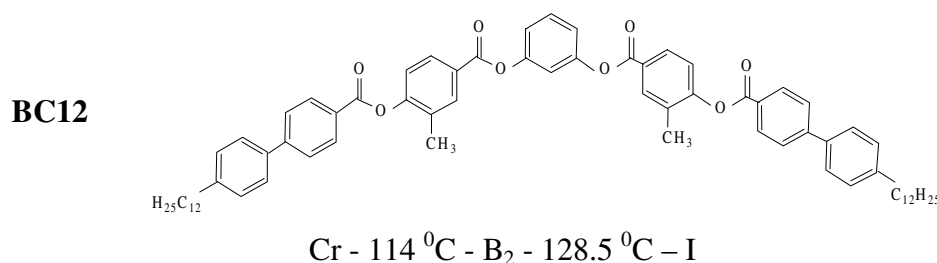
Cr - 114 ^0C - B_2 - 128.5 ^0C – I

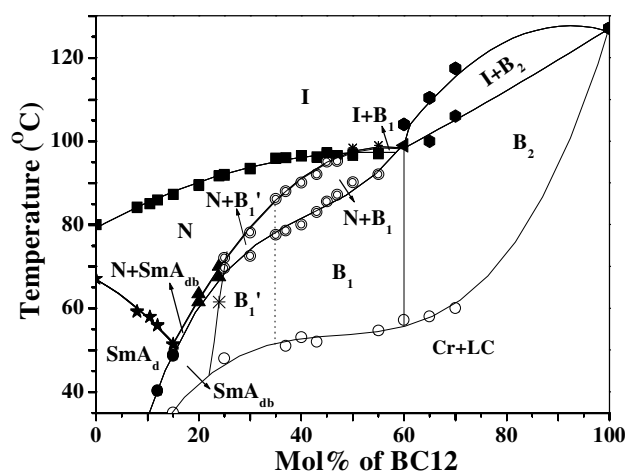Figure 5.11: Chemical structure and transition temperatures of the banana shaped compound BC12.

Figure 5.12: The concentration – temperature phase diagram of binary mixtures of BC12 and 8OCB reproduced from reference [2].

They propose that the mutual orientation of rod and banana shaped molecules in the SmA_{db} phase is as shown in Figure 5.13. The banana shaped molecules which are orientationally disordered in the uniaxial SmA_d phase become orientationally ordered in the background matrix of rods, the latter remaining intact at the transition from uniaxial SmA_d phase to *biaxial* SmA_{db} phase [2].
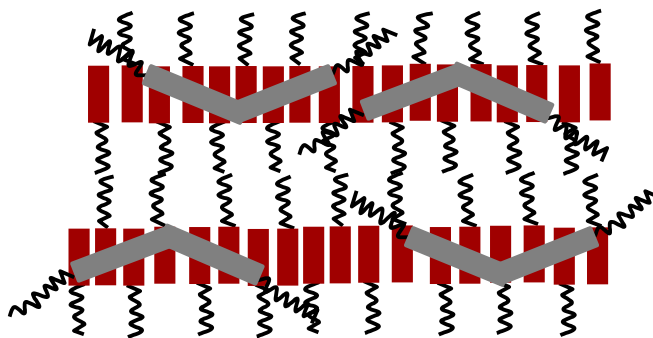

Figure 5.13: Schematic diagram of the arrangement of banana-shaped molecules and rod-like molecules in the SmA_{db} phase (reproduced from reference [2]).

We have monitored the transmitted intensity from a *homeotropically* aligned sample of a binary mixture with 14 mol% of BC12 mounted in the HP cell. The data at atmospheric pressure is shown in Figure 5.14.
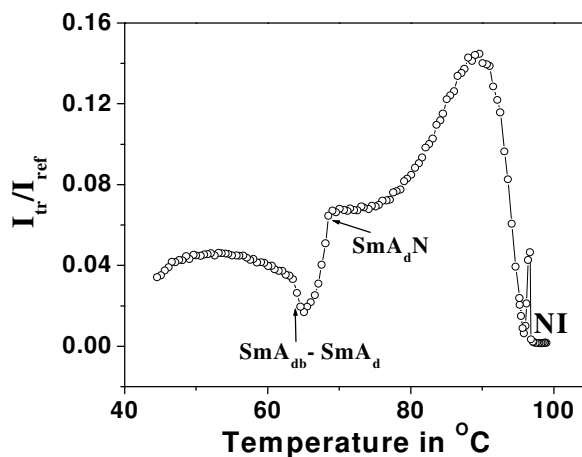
Figure 5.14: The temperature variation of the ratio of transmitted intensity to reference intensity from a *homeotropically* aligned sample of a binary mixture of 14 mol% of BC12 with 8OCB mounted in the HP cell at atmospheric pressure.

The small peak observed near the NI transition corresponds to the nematic-isotropic coexistence region. In the homeotropic geometry as the optic axis of the sample in the nematic phase is along the direction of propagation of the laser beam, the transmitted intensity of the sample placed between crossed polarisers is expected to be zero. As discussed in the previous chapter (see section 4.2) there will be strong scattering of light due to thermal fluctuations of the director in the uniaxial nematic phase. Hence the measured intensity in the uniaxial nematic phase seen in Figure 5.14 is the *scattered* intensity which is $\propto 1/K_{22}q^2$ [13], where K_{22} is the twist elastic constant. As the twist elastic constant K_{22} diverges near the N-SmA$_d$ transition point a drastic decrease in the scattered intensity can be observed (Figure 5.14). The residual intensity seen in this region may be due to some defects in the sample. At the SmA$_d$ - SmA$_{db}$ transition point the transmitted intensity increases (Figure 5.14) as the medium becomes biaxial and has birefringence along the viewing direction.

The binary mixture with 14 mol% of BC12 taken between an ordinary glass slide and a coverslip observed under a polarising microscope exhibits the following phase transition sequence: I - 87.6 ^{0}C – N – 51.8 ^{0}C – SmA$_d$ - 48 ^{0}C - SmA$_{db}$. But it can be observed from Figure 5.14 that the phase transition sequence of the sample

mounted in the HP cell without an externally applied pressure is :I - 97 ^{0}C - N - 68.4 ^{0}C - SmA$_d$ - 64.6 ^{0}C - SmA$_{db}$. The sample is mounted in the liquid crystalline phase in the HP cell. Hence on heating the sample the pressure in the sample raises leading to increase in transition temperatures as discussed in section 5.34. Comparing the difference between the NI transition temperatures the estimated *excess* pressure is ~ 250 bars at ~ 97 ^{0}C.
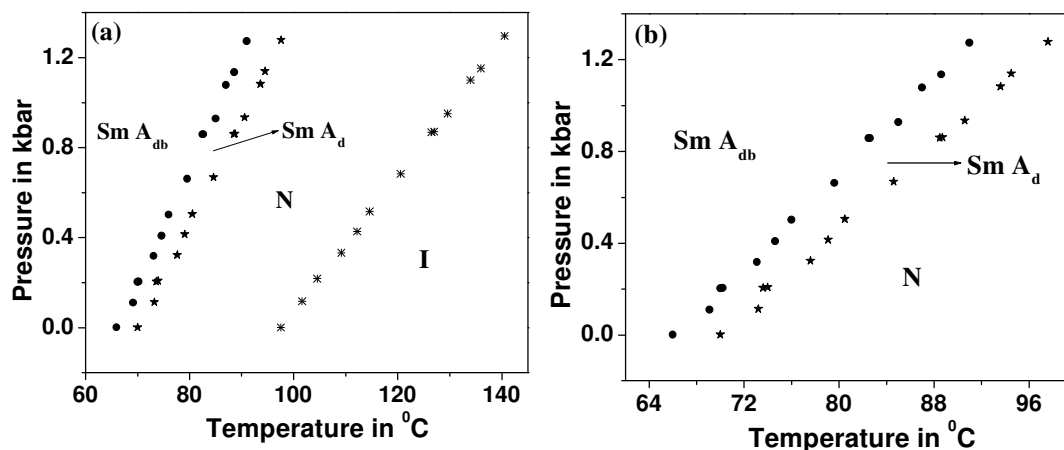

Figure 5.15: The Pressure-temperature phase diagram of a binary mixture of 14 mol% of BC12 with 8OCB (the values of pressure indicated in the diagram correspond to the *line pressure*).

The P-T phase diagram of the above binary mixture is shown in Figure 5.15 in which NI, SmA$_d$-N, SmA$_{db}$-SmA$_d$ transition temperatures are plotted as functions of applied pressure (line pressure). The uniaxial SmA$_d$ range in the absence of external applied pressure is ~ 4 ^{0}C, and is enlarged only to ~ 6.5 ^{0}C at an applied external pressure of ~ 1300 bars. The value of dP/dT$_{NI}$=30 bar/^{0}C is comparable to the value of a typical pure calamitic liquid crystal as the concentration of the rod like molecule (8OCB) in this binary mixture is high. The values of dP/dT at SmA$_d$-N, SmA$_{db}$-SmA$_d$ transitions are 46 bar/^{0}C and 51.6 bar/^{0}C respectively. The major component of the mixture, 8OCB in the pure form shows a nonlinear behaviour for SmA$_d$-N transition in the P-T plane (See Figure 2.15) and the SmA$_d$ phase gets bounded at a pressure of about ~ 2.3 kbar and already at ~ 1 kbar, the PT line has a curvature. However, we do not observe such a non-linear behaviour for SmA$_d$-N transition in the P-T plane in this mixture.

5.36 P-T phase diagram of 7(CN)5

The liquid crystal 7(CN)5 is known to exhibit Smectic-C like (cybotactic) short range ordering throughout the nematic range [4]. The molecule has a cyano group which is at an angle of ~60^0 with the long axis of the molecule (see Figure 5.16). Madhusudana and co-workers have reported that the thermal variation of the refractive index μ_o of this compound shows a broad minimum at a temperature of ~ T_{NI}-12 ^0C and at low temperatures the value of μ_o increases which is an unexpected behaviour [4]. However, the extraordinary refractive index μ_e increases with decreasing temperature as expected. They also report that the tilt angle of cybotactic structure θ decreases from ~ 48^0 to 40^0 on increasing the temperature from ~ 25 to 90 ^0C. The rate of variation of θ increases with increasing temperature.
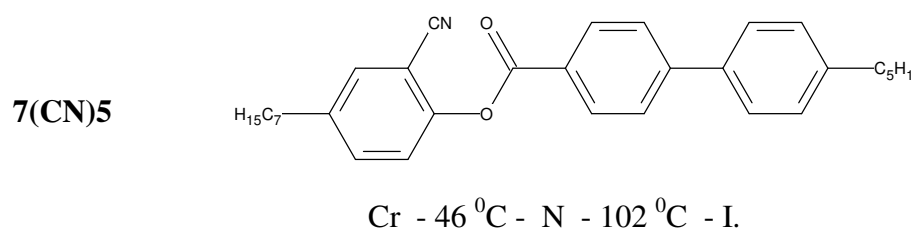

7(CN)5

Cr - 46 ^0C - N - 102 ^0C - I.

Figure 5.16: Chemical structure and transition temperatures of 7(CN)5.

We have carried out the optical path difference measurements on a planar aligned sample of this compound at various pressures with the motivation of observing a possible smectic C (SmC) phase at elevated pressures. The transmitted intensity data from measurements at pressures of   ~560 bars and ~800 bars are presented in Figure 5.17. It can be noticed that there is a jump in the intensity at ~ 61.4 ^0C at a pressure of ~560 bars (Figure 5.17b) indicating a phase transition. And a jump can be noticed at   ~64.9 ^0C at a pressure of ~800 bars (Figure 5.17d). The temperature at which the jump is observed increases with increasing pressure.
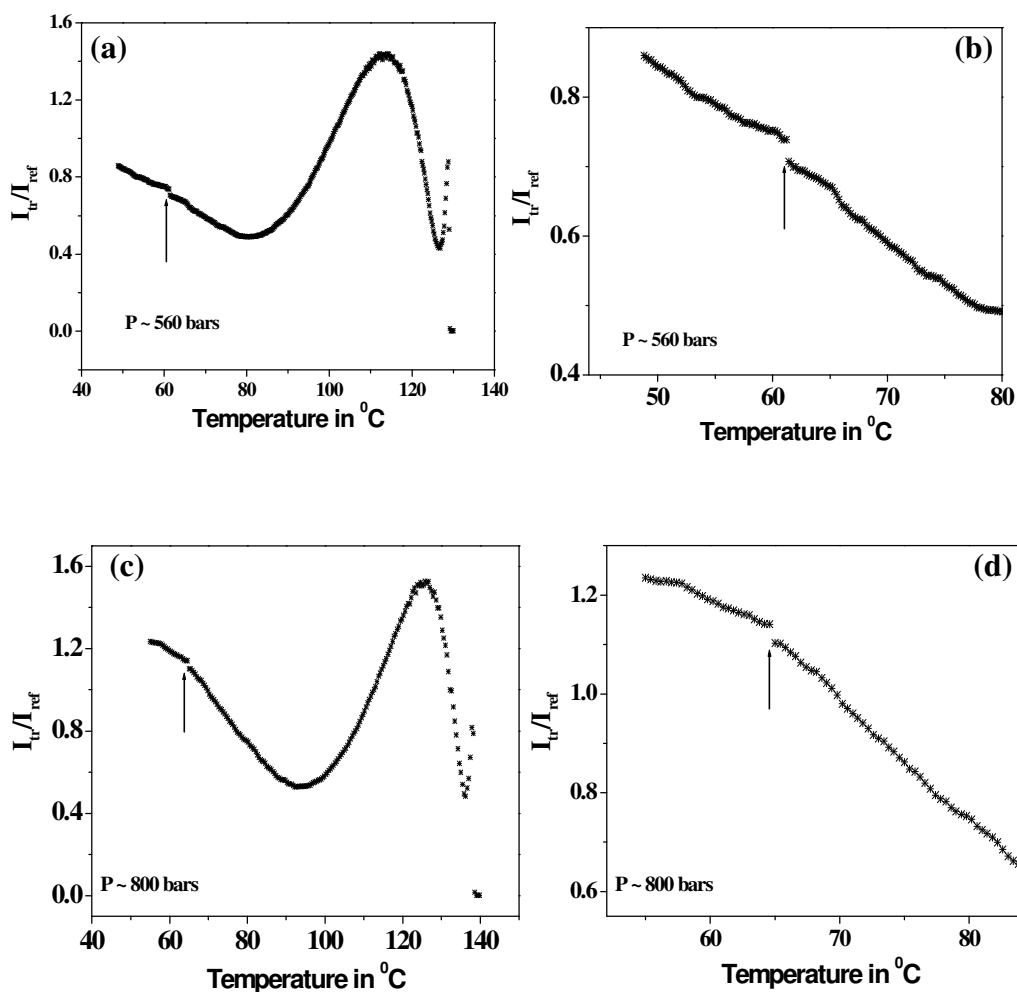
Figure 5.17: The ratio of transmitted intensity to reference intensity as a function of temperature for 7(CN)5 at pressures of ~560 bars and ~800 bars: (a) and (c) over the entire nematic range; (b) and (d) on an expanded temperature scale around the jump in tranmitted intensity.

On observing the sample under the microscope (section 2.2, Figure 2.8) we could not detect any textural changes around the temperature at which the jump in the intensity is observed. We cannot assert that the low temperature phase is the SmC phase. Due to some leakage of the oil into the sample we have not been able to carry out experiments at pressures >1.2 kbar. The P-T phase diagram is shown in Figure 5.18. The dP/dT at NI transition is 23.4 bar/^{0}C. The dP/dT of the *pressure induced transition* is ~ 47 bar/^{0}C.
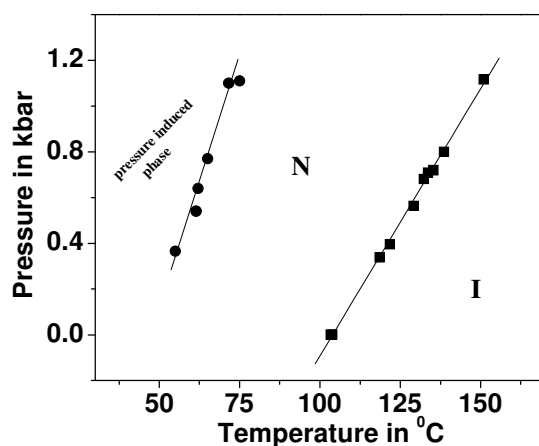
Figure 5.18: The pressure – temperature phase diagram of 7(CN)5.

5.37 P-T phase diagram of a binary mixture of a chiral and an achiral compounds exhibiting twist grain boundary phases

The compound CE8 is chiral in nature and exhibits a variety of phase transitions (Figure 5.19). As mentioned in section 5.1 the binary mixture of 7(CN)5 and the chiral compound CE8 (Figure 5.19) exhibits TGB phases in a certain range of concentrations of 7(CN)5. The temperature range of TGB_A phase increases with the increasing concentration of the *nonchiral* compound 7(CN)5. Above 34 wt% of 7(CN)5 the $UTGB_C^*$ phase is observed (Figure 5.20) [3].

CE8

Cr - 67 ^{0}C - SmI* - 70 ^{0}C - SmC^{*-} 80.5 ^{0}C - SmA - 136.5 ^{0}C - N*

- 138.8 ^{0}C - BP2 - 139.7 ^{0}C - BP1 - 140.5 ^{0}C I.
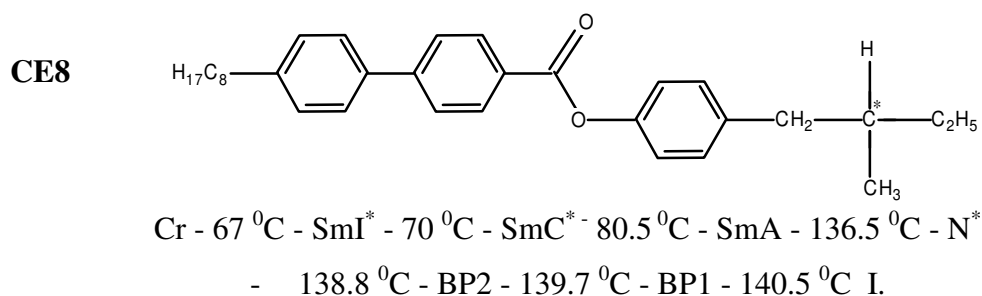
Figure 5.19: Chemical structure and transition temperatures of chiral compound CE8. The * indicates chirality.
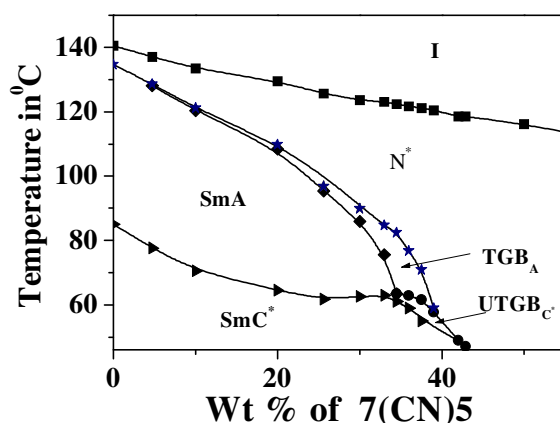
Figure 5.20: Part of the phase diagram containing the TGB phases in binary mixtures of CE8 and 7(CN)5 (adapted from reference [3]).

Only a couple of high pressure studies on systems exhibiting TGB_A phases are reported in the literature [14-16]. Krishna Prasad et al [14] have reported that binary mixtures of CE8 with 4-n-dodecyloxy biphenyl-4′-(2′-methyl butyl) benzoate (C12) in a certain range of concentrations exhibit the phase sequence: I – cholesteric (N*) - TGB_A-SmA-SmC*. They have carried out HP measurements on a few mixtures and in one of them, they could induce the TGB_A phase at high pressures. Maeda et al [15] have studied the effect of pressure on the phase behaviour of a dimesogenic liquid crystalline compound exhibiting the TGB phase using a wide angle X-ray scattering technique. However due to the high values of N*-TGB and TGB-SmC* transition temperatures they have not presented the P-T behavior of these transitions.

For the TGB_A phase to form, the Landau Ginzburg parameter $\kappa=\lambda/\xi$ must satisfy $\kappa > 2^{-1/2}$, where λ is the penetration depth for twist deformation and ξ is the smectic order parameter coherence length [13]. Carboni et al [16] have reported the P-T phase diagram of a pure compound exhibiting the phase sequence: I-TGB_A-SmC*. The slopes of both the phase boundary lines in the P-T phase diagram are negative. They interpret this trend by assuming an increase in volume at the transition to a more ordered phase. They report that the stability of the TGB_A phase is reduced at high pressures and the phase does not exist above ~250 bars. They speculate that the disappearance of TGB_A phase at high pressures indicates that the Ginzburg parameter κ decreases with increasing pressure.
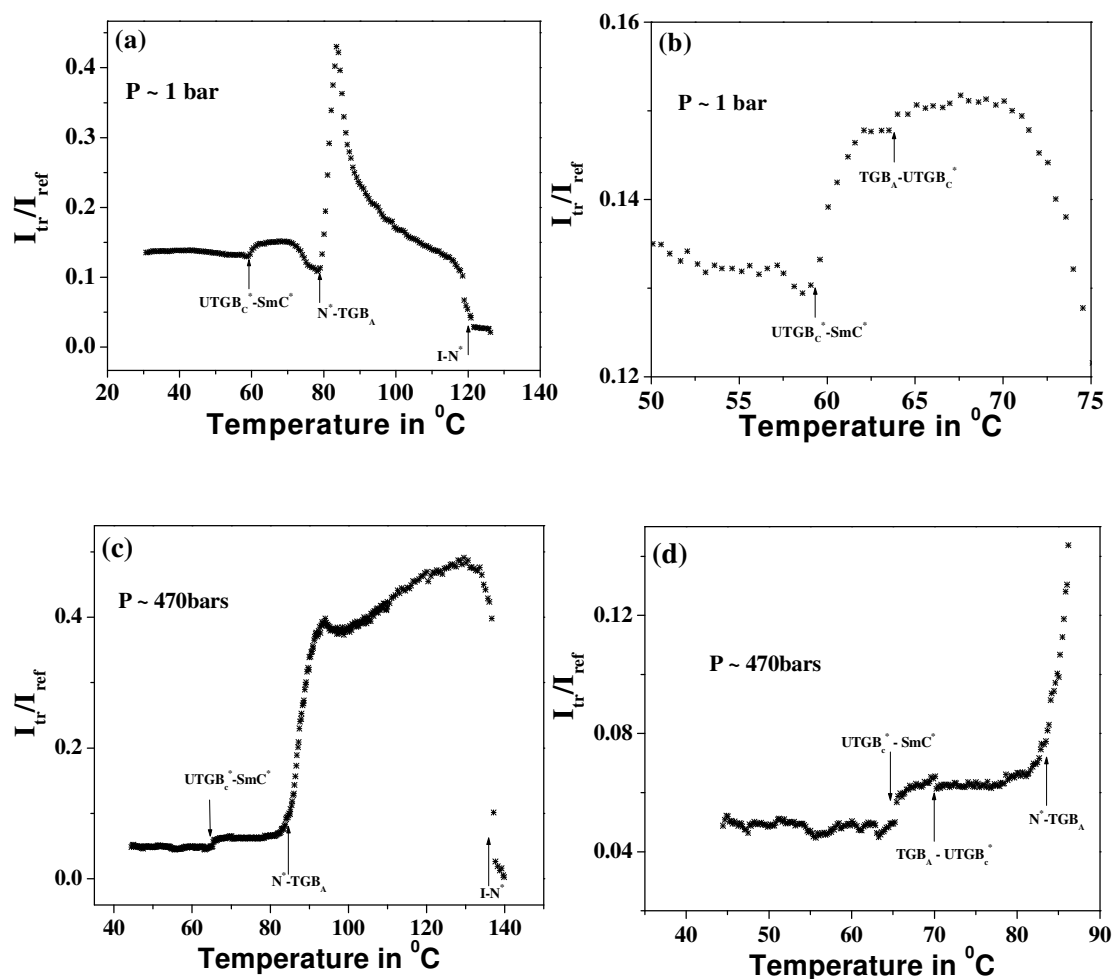
Figure 5.21: The temperature variation of the ratio of transmitted intensity to reference intensity from a planar aligned sample of 36 wt% of binary mixture of 7(CN)5 with CE8 at atmospheric pressure as well as at ~ 470 bars: (a) and (c) over the entire temperature range, (b) and (d) over a narrow range of temperatures around the mesophase transitions including TGB phases.

The binary mixture with 36 wt% of 7(CN)5 exhibits the following phase transition sequence: I - 121.6 ^{0}C - N* - 78.6 ^{0}C - TGB$_A$ - 63 ^{0}C - UTGB$_c^*$ - 59.3 ^{0}C - SmC*. We have carried out the measurement of optical intensity of a planar aligned sample of the above mixture placed between crossed polarisers for detecting the phase transition temperatures at various pressures. The data at atmospheric pressure as well as at a pressure of ~ 470 bars are shown in Figure 5.21.
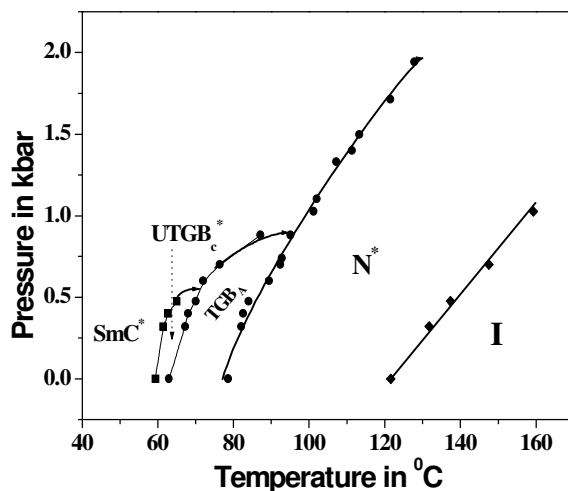
Figure 5.22: The pressure-temperature phase diagram of a binary mixture of 36 wt% of 7(CN)5 with CE8.

We have constructed the P-T phase diagram using the transition temperature data along various isobars and is shown in Figure 5.22. The value of dP/dT_{N^*I} ~ 26.6 bar/^{0}C. The TGB$_A$ phase gets bounded at a pressure ~ 900 bars. The UTGB$_c^*$ phase gets bounded at an even lower pressure of ~ 600 bars. The disappearance of the TGB phases at high pressures probably indicates that the Ginzburg parameter κ decreases with increasing pressure.

5.4   Conclusions

We have reported the P-T phase diagrams of various liquid crystalline systems. We have found that an *excess pressure* is generated when a sample in the fluid state is mounted in the high pressure cell as the volume is fixed. In a pure nematogen known to exhibit a skewed cybotactic type of short range order at atmospheric pressure we have found a liquid crystal-liquid crystal transition at elevated pressures. We have presented the P-T phase diagram of a binary mixture exhibiting TGB phases, in which the TGB phases get bounded at elevated pressures.

References

1. R. Pratibha, N. V. Madhusudana and B.K. Sadashiva, "An orientational Transition of Bent-Core Molecules in an Anisotropic Matrix", *Science*, **288**, 2184-2187, 2000.

2. R. Pratibha, N.V. Madhusudana and B.K. Sadashiva**, "**Two-dimensionally periodic phases in mixtures of compounds made of rod-like and bent-core molecules", (accepted for publication in *Phys. Rev. E*).

3. P.A. Pramod, R. Pratibha and N.V. Madhusudana, "A three dimensionally modulated structure in a chiral smectic-C liquid Crystal", *Curr. Sci*. **73**, 761-765, 1997.

4. N.V. Madhusudana, K.P.L. Moodithaya and K.A. Suresh, "Effect of Skew Cybotactic Structure on the optical Properties of a Nematogen with a Lateral Cyano Substituent", *Mol. Cryst. Liq .Cryst*. **99**, 239-247, 1983.

5. A Wiegeleben, H.J. Deutscher, D. Demus and H. Altmann, "Kalorimetrische Untersuchungen an kristallin-fluessigen trans-4-n-Alkylcyclohexancarbonsaeure-(4-cyanophenylestern)", *Z. Chem.* **21**, 28, 1981.

6. M. Takahashi, S. Mita and S. Kondo, " Study on Molecular Polarizabilities of Cyclohexane Derivatives", *Mol. Cryst. Liq.Cryst*. **132**, 53-64, 1986.

7. P.P Karat and N.V. Madhusudana, "Elastic and Optical Properties of some 4′-n-Alkyl-4-cyanobiphenyls" *Mol.Cryst. Liq. Cryst*. **36**, 51-64, 1976. (for 8CB); S.Sen, P. Brahma, S.K. Roy, D.K. Mukherjee and S.B. Roy, "Birefringence and Order Parameter of Some Alkyl and Alkoxycyanobiphenyl Liquid Crystals", *Mol. Cryst. Liq. Cryst*. **100**, 327-340, 1983 (for 8OCB). (The density of MCB is estimated as an appropriate average, using the mole fractions of 8CB and 8OCB).

8. D. Guillon, P.E. Cladis and J. Stamatoff, "X-Ray study and Microscopic study of the Reentrant Nematic Phase", *Phys. Rev. Lett*. **41**, 1598-1601, 1978.

9. A.R. Kortan, H.V. Kanel, R.J. Birgeneau and J. D. Litster, "High-Resolution X-Ray scattering study of the Nematic-Smectic A- Reentrant Nematic transitions in 8OCB/6OCB Mixtures", *Phys. Rev. Lett.* **47**, 1206-1209, 1981.

10. P. E. Cladis, D. Guillon, F. R. Bouchet and P. L. Finn, "Reentrant nematic transitions in cyano-octyloxybiphenyl (8OCB)", *Phys. Rev. A.* **23**, 2594-2601, 1981.

11. Surajit Dhara and N.V. Madhusudana, "Enhancement of orientational order parameter of nematic liquid crystals in thin Cells", *Eur. Phys. J.E.* **13**, 401- 408, 2004.

12. S. Chandrasekhar, *Liquid Crystals*, Cambridge University Press, Cambridge, 1992.

13. P. G. de Gennes and J. Prost, *The Physics of Liquid Crystals*, Clarendon Press, Oxford, 1993.

14. S. Krishna Prasad, Geetha G. Nair, S. Chandrasekhar and J.W. Goodby, "Pressure induced twist grain boundary phase", *Mol. Cryst. Liq. Cryst.* **260**, 387-394, 1995.

15. Yoji Maeda, Yong-Kuk Yun and Jung-il Jin, "Effect of pressure on phase behavior of a dimesogenic liquid crystal compound", *Mol. Cryst. Liq. Cryst.* **280**, 85-90, 1996.

16. C. Carboni, H. F. Gleeson, J. W. Goodby and A. J. Slaney, "A specialized apparatus for the study of liquid crystals at high pressures", *Liq. Cryst.* **14**, 1991-2000, 1993.